JABFM
eISSN 2280-8000

J Appl Biomater Funct Mater 2017; 15 (Suppl 1): S1-S6
DOI: 10.5301/jabfm.5000341

ORIGINAL RESEARCH ARTICLE

Open Access

Facile synthesis of reduced graphene oxide/Fe_3O_4 nanocomposite film

Cunqing Ma[1], Kaiyu Yang[2], Lili Wang[3], Xin Wang[1]

[1] Key Laboratory of Automobile Materials of MOE, College of Materials Science and Engineering, Jilin University, Changchun - PR China
[2] College of Automotive Engineering, Jilin University, Changchun - PR China
[3] College of Science, Changchun University, Changchun - PR China

ABSTRACT

Background: This study aims at proposing a facile method to prepare rGO/Fe_3O_4 composite film with adjusted magnetic properties and electronic conductivity.

Methods: Colloidal solution of graphene oxide (GO)/Fe_3O_4 nanoparticles (F-NPs) with a size in the range of 20-80 nm were prepared by a solution-blending method and heated step-by-step from room temperature to 60°C, 120°C and 160°C for 12 hours, respectively, to obtain a reduced graphene oxide (rGO)/F-NP composite film. The structure, morphology, components, magnetic properties and electrical conductivity of the composite films were characterized by X-ray diffraction, scanning electron microscopy, Fourier transform infrared spectroscopy, X-ray photoelectron spectroscopy, Raman spectroscopy, superconducting quantum interference devices and 4-probe instrument.

Results: The results indicated that the F-NPs were uniformly distributed on the graphene film, and the composite exhibited good ferromagnetic properties and conductivity, which could be adjusted easily via different loadings of F-NPs. A high content of F-NPs (200 mg) led to a strong saturation magnetization of 63.6 emu·g^{-1}, with a coercivity of about 104.9 oersted (Oe). Whereas a high conductivity of 6.5 S·m^{-1} was obtained at low amounts of F-NPs (40 mg). Notably, rGO/Fe_3O_4 composite film fabricated by this simple method is widely used in various fields including magnetoelectronics, electrochemical energy conversion and storage, and magnetic nanodevices and others.

Conclusions: A graphene-based film deposited by Fe_3O_4 nanoparticles with controllable loadings has been fabricated by a step-by-step heating treatment of GO/Fe_3O_4 colloidal solution.

Keywords: Composite film, Electrical conductivity, Fe_3O_4 nanoparticles, Magnetic properties, Reduced graphene oxide

Introduction

Because of its extraordinary 2-dimensional structure and very high specific surface area (2,630 $m^2 \cdot g^{-1}$), graphene exhibits unique physicochemical properties that have attracted much attention since Geim and Novoselov of the University of Manchester obtained monolayer graphene by exfoliating graphite using a mechanical method (1-4). Currently, the method for producing graphene materials such as graphene oxide (GO) flakes, graphene films and graphene nanoplatelets has been extended to exfoliating graphite using chemical methods and chemical vapor deposition (CVD) on various substrates (5-7). It has been demonstrated that these 3 main types of graphene materials can be used as nanofillers for possible applications in paints, coatings and nanocomposites or as a support to load some kinds of metals or metal oxide/hydroxide including Fe_3O_4 nanoparticles (7).

As a magnetic material, Fe_3O_4 has been widely applied to the sensor (8), biomedicine (9), magnetic storage (10), pollution treatment (11), food detection (12) and other fields because of its low toxicity, high biocompatibility and high catalytic activity etc. Special attention has recently been paid to graphene/Fe_3O_4 composite film since the creation of a synergistic effect might be expected to have great potential in lithium ion batteries, microwave-absorbing materials, biomedicine and supercapacitors (13-16). Until now, a variety of methods have been explored to prepare graphene/Fe_3O_4 composites, including the hydrothermal/solvothermal method, microwave-assisted synthesis, the sol-gel method, the in situ self-assembly method and the off-site hybrid method. Using the solvothermal method at 220°C for 30 minutes, He and Gao (17) prepared a GO/Fe_3O_4 mixture that was reduced by NaOH/DEG solution at 220°C for 1 hour. The as-prepared rGO/Fe_3O_4 solution was then vacuum-filtered to form a

Accepted: January 13, 2017
Published online: April 20, 2017

Corresponding author:
Prof. Xin Wang
College of Materials Science and Engineering
Key Laboratory of Automobile Materials of MOE
Jilin University
Qianjin Street 2699
130012 Changchun, China
wang_xin@jlu.edu.cn

composite film. After careful measurement, the electrical conductivity of the film was found to be 0.7 $S \cdot m^{-1}$, and the saturation magnetization value was in the range of 0.5 to 44.1 $emu \cdot g^{-1}$ when the content of Fe_3O_4 was 5.3% to 57.9%, with the average diameter of the nanoparticles changing from 1.2 to 6.3 nm (17). Liang et al filtered rGO/Fe_3O_4 nanoparticle dispersion that has been prepared by chemical reduction method to synthesize graphene-based films. Their graphene/F-NP hybrid films exhibited superparamagnetic properties for potential applications as magnetic-controlled switches (18). Also, Narayanan et al reported using a chemical coprecipitation technique to synthesize uniformly sized Fe_3O_4 nanoparticles (range 10-15 nm) then mixed with GO suspension to get GO/Fe_3O_4 freestanding membranes by vacuum filtering. After that, the film was peeled off the filter paper and treated with 2-M hydrazine monohydrate at 90°C for 1 hour to fabricate rGO/Fe_3O_4 film (19). Even though graphene/Fe_3O_4 composite film has been extensively investigated for the last few years, finding a relatively facile method and a controlled size of Fe_3O_4 NPs on graphene still remain major challenges (17).

In this work, we used an improved thermal treatment method without adding any reducing agent, to prepare rGO/F-NP nanocomposite film. Namely, GO/Fe_3O_4 colloid solution prepared by the solution-blending method was heated step-by-step from room temperature to 160°C to fabricate reduced GO film instead of annealing directly up to a high temperature. The Fe_3O_4 nanoparticles were found to be well dispersed due to the existence of graphene sheets. Magnetic properties of the nanocomposite film can be controlled readily by altering the Fe_3O_4 nanoparticle feeding, and film thickness is dependent on the amount of GO/F-NP solution coated on a substrate. We demonstrated that rGO/F-NP films could be prepared by a low-temperature annealing treatment, which is expected to provide a simple and effective process for the preparation of graphene-based composite films.

Methods

Materials

Sulfuric acid (H_2SO_4, 99%; Beijing Chemical Works, China), hydrochloric acid (HCl, ≥37%; Beijing Chemical Works, China), potassium permanganate ($KMnO_4$, ≥99%; Beijing Chemical Works, China), hydrogen peroxide (H_2O_2, 30%; Beijing Chemical Works, China), sodium nitrate ($NaNO_3$, ≥99%; Sinopharm Chemical Reagent Co. Ltd., China), citric acid monohydrate ($C_6H_8O_7 \cdot H_2O$, ≥99.5%; Sinopharm Chemical Reagent Co. Ltd., China), natural powder graphite (325 mesh, 99.99%; Alfa Aesar) and magnetite (Fe_3O_4; Xiya Reagent) were acquired. All reagents were analytical grade and used without purification. Water was purified using ultrapure water equipment.

Sample preparation

We chose natural powder graphite to prepare a GO colloidal solution (20 $mg \cdot mL^{-1}$) using a modified Hummers' method (20). In brief, a blend of natural graphite powder (2 g) and $NaNO_3$ (1.5 g) was placed in cold (0°C) concentrated H_2SO_4 (69 mL), and then $KMnO_4$ (9 g) was added gradually and slowly with stirring. The mixture was placed in ice water for 12 hours and then heated to 35°C for 1 hour. The deionized water (200 mL) was added when the mixture had cooled to room temperature, after heating to 60°C for 18 hours. H_2O_2 was added dropwise until the solution became bright yellow, and then the solution was first washed by centrifugation with 10% hydrochloric acid solution for 3 times and then washed with deionized water to neutral to obtain the GO colloid solution. To prepare a composite film, 0 mg, 40 mg, 120 mg and 200 mg of Fe_3O_4 nanoparticles were dispersed respectively in 40 mL citric acid solution (0.5%) and sonicated for 5 minutes. Ten milliliters of colloid solution of GO and the as-prepared Fe_3O_4 nanoparticle dispersion were mixed and mechanically stirred for 20 minute to create the GO/F-NP colloidal solutions. Mixtures were transferred to glass dishes and placed in a vacuum oven, and then dried at 60°C, 120°C, and 160°C, for 12 hours, respectively. Finally, we obtained a flat and continuous rGO/F-NP composite film after the prepared samples cooled down to room temperature in the vacuum oven. The rGO/F-NP film could easily be peeled off from the glass for investigation. For comparison, pure rGO film was also prepared. A schematic of the process is shown in Figure 1. The rGO/F-NP freestanding films were prepared through 2 steps of solution blending and step-by-step heating. In the thermal reduction process of graphite oxide, the loss of the interstitial H_2O mainly occurred at 110°C (21). When the temperature was heated above 150°C, the functional groups of GO began to decompose with liberation of CO, CO_2 and H_2O (22). If the annealing time is increased, the reduction of GO will be better (23). In the case of rapid heating, the structure of GO will be destroyed to form a slight soot (22). Therefore, it is expected that to obtain a film without wrinkles and pores, a step-by-step process with slow heating needs to be used, although this is time consuming.

Characterization

The structure of the composite film was characterized by X-ray diffraction (XRD, D8tools; Bruker), and the component and carbon-bonding types were identified by Fourier transform infrared spectroscopy (FT-IR, Perkin Elmer Spectrum One B) and X-ray photoelectron spectroscopy (XPS, Thermo ESCALAB 250 spectrometer). The morphology was analyzed by scanning electron microscopy (SEM, JOEL JSM-6700F), the typical Raman spectra was measured by Raman spectroscopy (532 nm), the magnetic properties were tested by superconducting quantum interference devices (SQUIDs) and the resistance was tested by 4-probe instrument (Keithley, PCT-1B).

Results and discussion

Usually, heating GO film at temperatures above 150°C will lead to the pyrolysis of oxygen-containing functional groups and thus the formation of rGO film. However, the annealing process will probably disturb the structure of the GO film, and obvious crumpled or cracked morphology will appear due to the emission of large amounts of gas (22, 24). Figure 2A shows the macroscopic morphology of GO, rGO and rGO/F-NP (200 mg) films. The black GO and rGO films can be observed having no crumpled structures on the surface. By comparison, the GO film surface is smoother, even

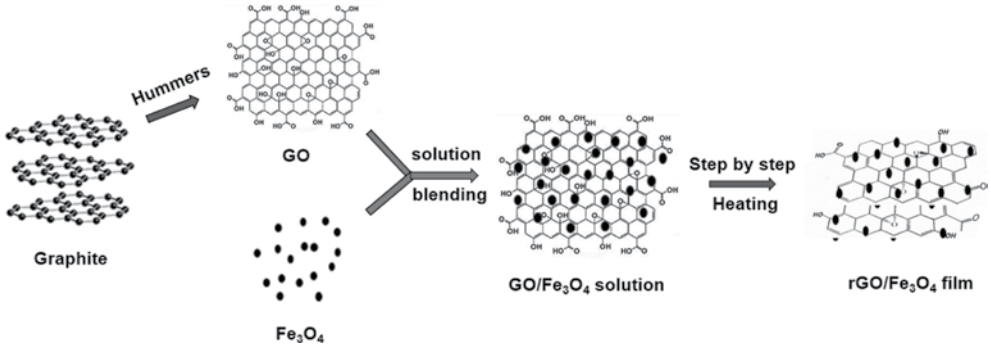

Fig. 1 - Synthesis scheme of reduced graphene oxide (rGO)/Fe_3O_4 nanoparticle (F-NP) composite film by a solution-blending method combined with an improved annealing treatment.

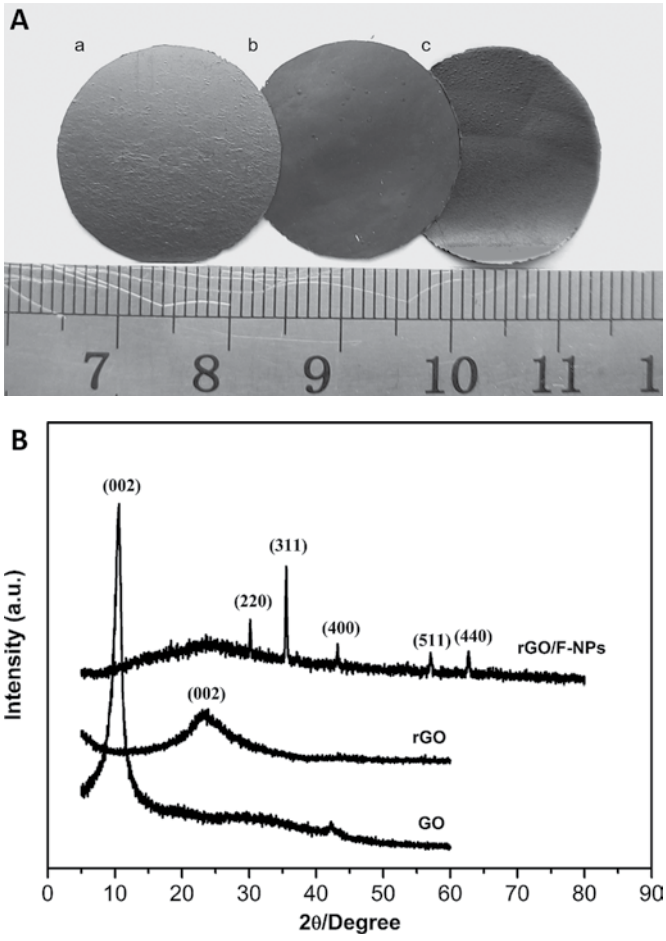

Fig. 2 - (**A**) Photographs of graphene oxide (GO) (a), reduced graphene oxide (rGO) (b) and rGO/ Fe_3O_4 nanoparticle (F-NP) (c) (200 mg) films; (**B**) their corresponding X-ray diffraction (XRD) patterns.

though after thermal treatment, the rGO and rGO/F-NP films still remain their integrity and continuous macroscopic structure, with only a small number of tiny pores on the surface of the composite film. We attributed the relatively smooth graphene-based composite film obtained, to the step-by-step thermal reduction process that may enable water molecules and oxygen-containing groups to be removed separately and slowly. Therefore the GO sheets get more of an opportunity to collide and link with each other through the hydrogen-bonding process to form a flat surface. The crystalline structure of the GO, rGO and rGO/F-NP composite film prepared was analyzed by XRD measurement (Fig. 2B). According to the standard XRD data for graphite (JCPDS card, file no. 41-1487), the characteristic diffraction peak at around 2θ = 26° has been replaced by a sharp peak at the position of 10.6° in the pattern for GO, indicating that the oxygen functional groups are inserted into the graphite layer. For the sample of rGO/F-NPs (200 mg), the positions and intensities of characteristic peaks can be clearly seen, which correspond well to the standard JCPDS card of magnetite (file no. 19-0629). The XRD pattern of rGO displays a low and broad characteristic peak between 20° and 30°, which indicates that GO is reduced to rGO in the reaction process, even though the crystallization has not been carried out very well. As the C(002) peak can hardly be seen for the composite sample in the XRD pattern, the graphene sheets might be deduced to have disordered stacking in the composites (25).

As seen in the representative SEM images shown in Figure 3A, the surface of rGO film presents the typical morphology of graphene with obvious wrinkle structures. In the SEM images of rGO/F-NP (200 mg) composite films with different NP contents (Fig. 3B-D), we can see that the surface of rGO loads uniformly small F-NPs with a size in the range of 20-80 nm. The size distribution of NPs mainly originates from the initial Fe_3O_4 powder material. The Fe_3O_4 nanoparticles in the composite have excellent dispersibility due to the existence of the graphene sheets and lower content of NPs. Figure 3B shows relatively sparsely attached to the surface of graphene film sheets, while with high content levels, the NPs are remarkably denser (Fig. 3D).

XPS was used to further investigate the crystal phase in rGO/F-NP (200 mg) composite films. In Figure 4A and B, the C1s spectra of rGO can be deconvoluted into 5 different peaks. The binding energies at 284.5, 285.8, 286.9, 288.3 and 289.2 eV have been assigned to the sp^2C = C, sp^3C-C, C-OH, C = O and O = C-OH groups, respectively; while 287.8 and 290.3 eV belong to C-O-C functional groups and corresponding π-π* vibration satellite peak, respectively. The C1s spectrum of rGO hardly changes after F-NPs are added, indicating that in using the solution-blending method for the preparation of rGO/F-NP composite, the attachment of NPs to rGO involves non-covalent bonding, which could be further confirmed by the FT-IR analysis that followed. The Fe 2p XPS spectrum of rGO/F-NP composite is given in Figure 4C. The weak binding energy peaks of Fe $2p_{3/2}$ and $2p_{1/2}$ suggest a small amount of Fe_3O_4

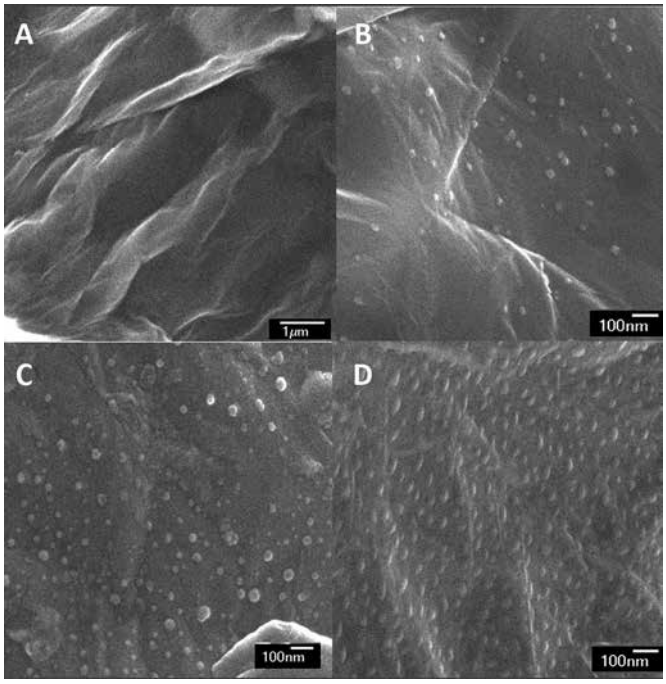

Fig. 3 - Scanning electron microscopy (SEM) images of reduced graphene oxide (rGO) (**A**) and rGO/Fe_3O_4 nanoparticle (F-NP) composite films with different contents of NPs: 40 mg (**B**), 120 mg (**C**) and 200 mg (**D**).

nanoparticles used in the composite samples. Figure 4D shows the O1s region of the prepared rGO/F-NP sample. Four different peaks centered at 532.0 eV, 533.0 eV, 533.8 eV and 531.0 eV are observed, corresponding to the C-O-C, H_2O, OH-O and O = C groups, respectively.

FT-IR analysis is shown in Figure 5A. The peak of GO at around 3,421 cm^{-1} can be attributed to the –OH stretching vibration, while 2 other peaks at 1,739 cm^{-1} and 1,626 cm^{-1} can be ascribed to the C = O stretching and C = C deformation vibration, respectively. The peaks at 1,171 cm^{-1} and 1,044 cm^{-1} belong to the C-O stretching vibration of the epoxy group and alkoxy (26). The absorption peaks of rGO and rGO/F-NP (200 mg) composite decrease or disappear significantly, showing that oxygen-containing groups are removed from the graphite oxide after heat treatment.

We used Raman spectral measurement to test the spectral characteristics of the GO/F-NP (200 mg) composite film before and after reduction. The results are shown in Figure 5B. We can clearly see that there are 2 characteristic peaks in the spectrum, which are the D band (1,349.9 cm^{-1}) and G band (1,589.2 cm^{-1}). The D band is related to the vibrations of sp^3 carbon atoms of disordered graphite, and the G band corresponds to the in hexagonal plane vibration of sp^2 carbon atoms (27). The intensity ratio of the D band and G band of GO/F-NP composite film (I_D/I_G) is increased to 1.57 from 1.13 after reduction, which proves that there are more numerous defects created during reduction of the GO/F-NPs (28).

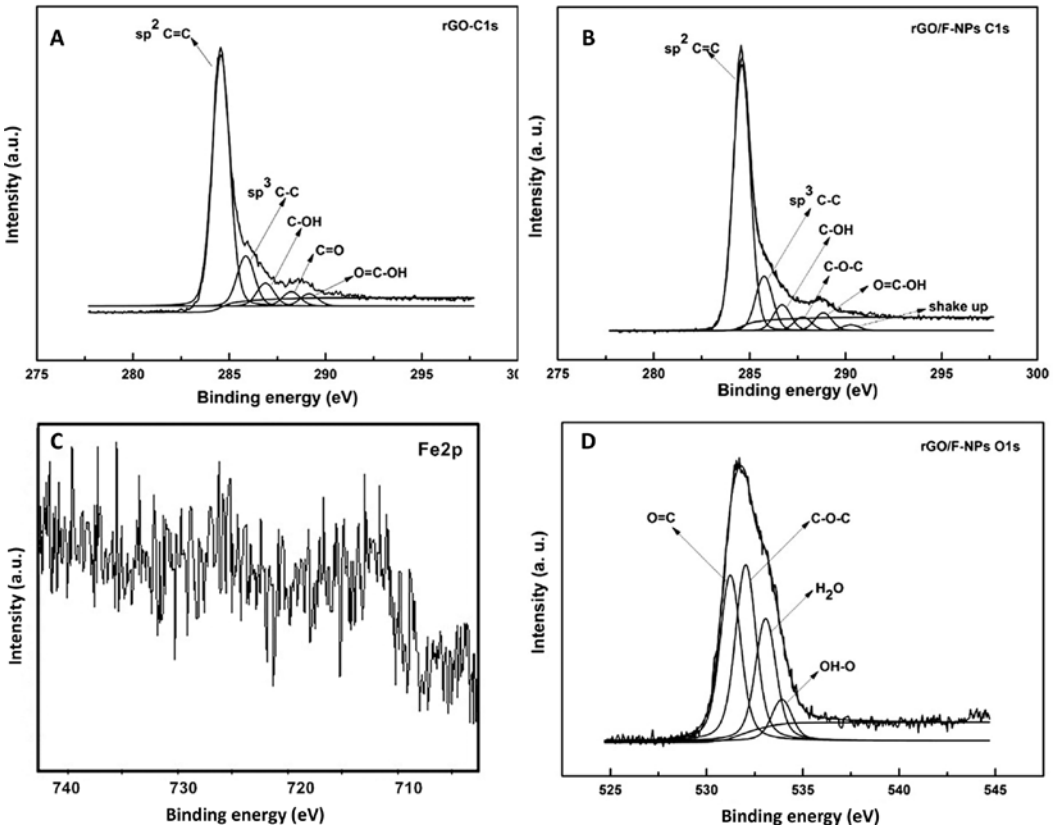

Fig. 4 - X-ray photoelectron spectroscopy (XPS) spectra of C1s for reduced graphene oxide (rGO) (**A**) and rGO/Fe_3O_4 nanoparticle (F-NPs) (**B**) (200 mg), and Fe2p (**C**) and O1s (**D**) for rGO/F-NPs (200 mg).

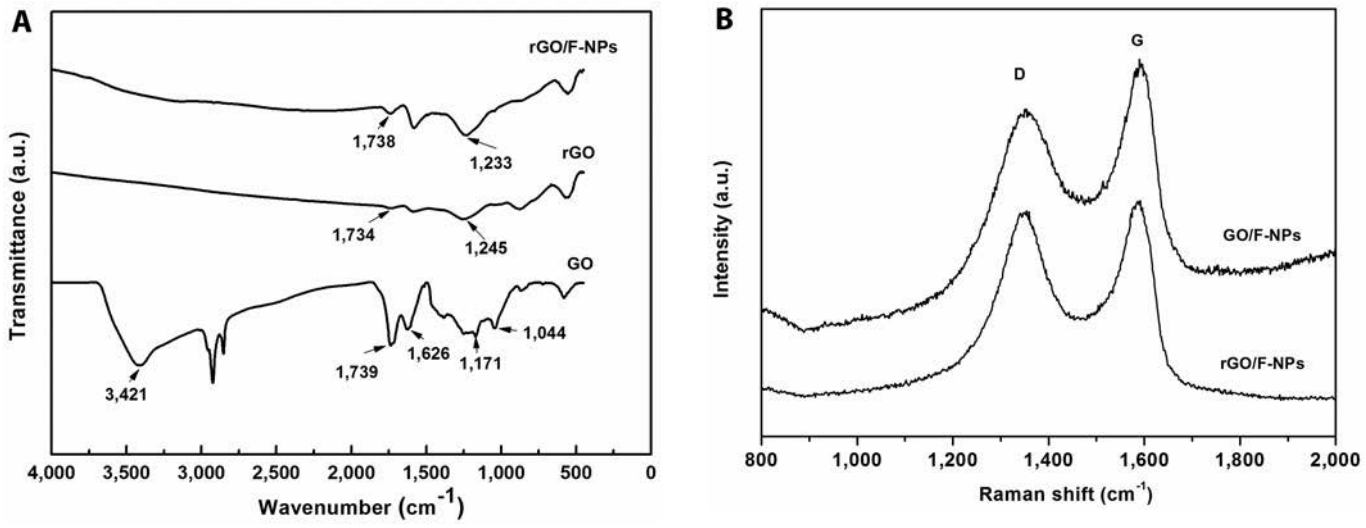

Fig. 5 - Fourier transform infrared (FT-IR) spectra of graphene oxide (GO), reduced graphene oxide (rGO) and rGO/Fe_3O_4 nanoparticle (F-NP) (200 mg) (**A**) composite films; and Raman spectra of the GO/F-NP (200 mg) and rGO/F-NP (200 mg) (**B**) composite films.

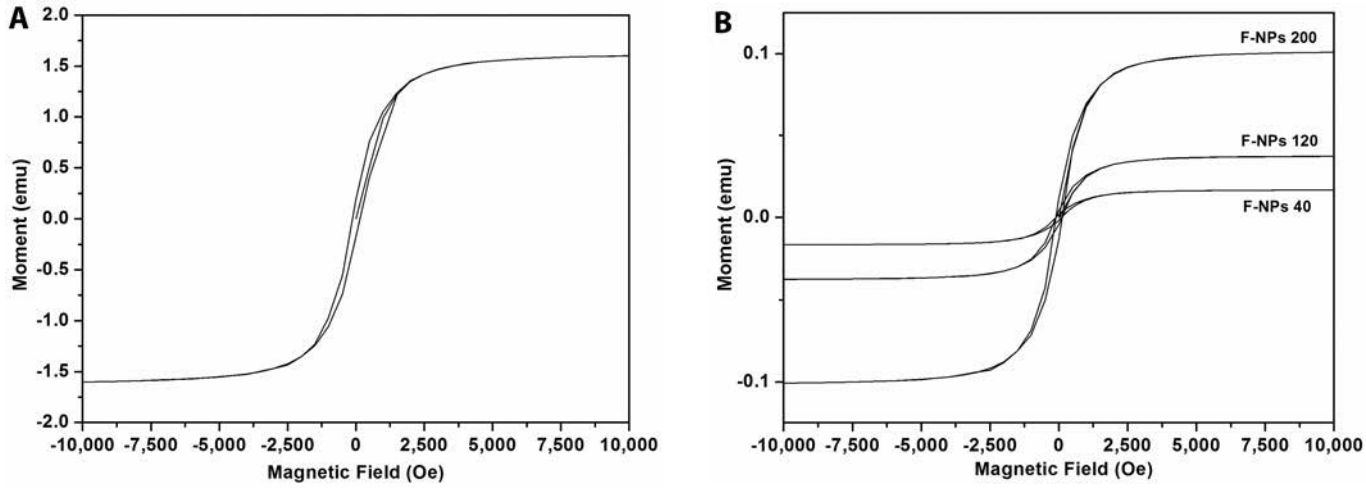

Fig. 6 - Magnetic hysteresis loops of Fe_3O_4 nanoparticle (F-NP) (**A**) and reduced graphene oxide (rGO)/F-NP (**B**) composite films.

The magnetic properties of pure F-NPs and rGO/F-NP composite with different contents were tested by SQUIDs (Fig. 6). The saturation magnetization and coercivity of the F-NPs was about 91.6 emu·g^{-1} and 126.3 oersted (Oe), respectively. As to the rGO/F-NP composites, the values of saturation magnetization were calculated to be about 63.6 emu·g^{-1} (3.0 mg), 37.5 emu·g^{-1} (1.6 mg) and 5.5 emu·g^{-1} (1.0 mg), while the value of coercivity remained unchanged at about 104.9 Oe. It can be seen that the saturation magnetization of the composites was largely dependent on the loading of the Fe_3O_4 nanoparticles, and a high value of 63.6 emu·g^{-1} was obtained by adding 200 mg of F-NPs. The unchanged coercivity for the composite with different amounts of Fe_3O_4 nanoparticles indicated that graphene-based film did not change F-NP anisotropy field – namely, the soft magnetic property was not changed much.

The conductivity of the rGO/F-NP composite films is shown in Table I, as measured by the 4-probe method. The results proved that the composite films had good conductivity. It is worth nothing that the films' conductivity gradually decreased with increasing Fe_3O_4 content because the conductivity of Fe_3O_4 nanoparticles is lower than that of graphene sheets (16). When the content of Fe_3O_4 was 40, 120 or 200 mg, the corresponding conductivity was 6.5, 5.1 and 4.3 S·m^{-1}, respectively, which was higher than that of the film of He and Gao (0.7 S·m^{-1}) which was prepared by chemical reduction (17). We attributed the higher conductivity to the direct and gentle thermal reduction of functional oxygen groups that facilitated the effective maintenance of the structural integrity of the composite films (29).

TABLE I - Electric conductivity of reduced graphene oxide/F-NP composite films

Fe_3O_4 contents (mg)	Resistivity (Ω^{-1})	Conductivity ($S \cdot m^{-1}$)
40	90.8	6.5
120	136	5.1
200	201.4	4.3

F-NP = Fe_3O_4 nanoparticle.

Conclusions

We prepared rGO/Fe_3O_4 NP magnetic composite films step-by-step by heating the colloidal solution of GO/Fe_3O_4 without using any chemical reduction agent. The slow thermal treatment proved to be effective in obtaining free-standing graphene-based composite film free from crack structures on the surface. The results showed that rGO/F-NP (200 mg) composite film has a high saturation magnetization of 63.6 $emu \cdot g^{-1}$, with coercivity of 104.9 Oe, and a good conductivity of 6.5 $S \cdot m^{-1}$ (40 mg). This simple, controllable and low-cost synthesis method makes it possible for graphene-based film to be used in many fields, including as supercapacitors, lithium ion batteries, environmental pollution treatments, sensors, microwave-absorbing materials and so on. Compared with rGO/F-NP film that has been prepared by directly heating a GO/F-NP solution up to 160°C, the slow thermal reduction approach turned out to be effective for a freestanding film with small amounts of tiny pores and free from crack structures on the surface.

Disclosures

Financial support: This project was sponsored by the National Natural Science Foundation of China (grant no. 51302019), the Natural Science Foundation of Jilin Province (grant no. 20150101029JC) and China Scholarship Council (CSC) for Xin Wang, a visiting scholar.
Conflict of interest: None of the authors has any financial interest related to this study to disclose.

References

1. Novoselov KS, Geim AK, Morozov SV, et al. Electric field effect in atomically thin carbon films. Science. 2004;306(5696):666-669.
2. Geim AK, Novoselov KS. The rise of graphene. Nat Mater. 2007;6(3):183-191.
3. Li D, Kaner RB. Materials science: graphene-based materials. Science. 2008;320(5880):1170-1171.
4. Kane CL. Materials science: erasing electron mass. Nature. 2005;438(7065):168-170.
5. Chen JH, Jang C, Xiao S, Ishigami M, Fuhrer MS. Intrinsic and extrinsic performance limits of graphene devices on SiO_2. Nat Nanotechnol. 2008;3(4):206-209.
6. Balandin AA, Ghosh S, Bao W, et al. Superior thermal conductivity of single-layer graphene. Nano Lett. 2008;8(3):902-907.
7. Zurutuza A, Marinelli C. Challenges and opportunities in graphene commercialization. Nat Nanotechnol. 2014;9(10):730-734.
8. Wu S, Wang H, Tao S, et al. Magnetic loading of tyrosinase-Fe_3O_4/mesoporous silica core/shell microspheres for high sensitive electrochemical biosensing. Anal Chim Acta. 2011;686(1-2):81-86.
9. Sun HW, Zhu XJ, Zhang LY, Zhang Y, Wang DQ. Capture and release of genomic DNA by PEI modified Fe_3O_4/Au nanoparticles. Materials Science & Engineering: C: Materials for Biological Applications. 2010;30(2):311-315.
10. Chen J, Ye X, Oh SJ, Kikkawa JM, Kagan CR, Murray CB. Bistable magnetoresistance switching in exchange-coupled $CoFe_2O_4Fe_3O_4$ binary nanocrystal superlattices by self-assembly and thermal annealing. ACS Nano. 2013;7(2):1478-1486.
11. Farrukh A, Akram A, Ghaffar A, et al. Design of polymer-brush-grafted magnetic nanoparticles for highly efficient water remediation. ACS Appl Mater Interfaces. 2013;5(9):3784-3793.
12. Ding N, Yan N, Ren C, Chen X. Colorimetric determination of melamine in dairy products by $Fe_{(3)}O_{(4)}$ magnetic nanoparticles-$H_{(2)}O_{(2)}$-ABTS detection system. Anal Chem. 2010;82(13):5897-5899.
13. Zhou GM, Wang DW, Li F, et al. Graphene-wrapped Fe_3O_4 anode material with improved reversible capacity and cyclic stability for lithium ion batteries. Chem Mater. 2010;22(18):5306-5313.
14. Zhang H, Xie AJ, Wang CP, Wang HS, Shen YH, Tian XY. Room temperature fabrication of an RGO-Fe_3O_4 composite hydrogel and its excellent wave absorption properties. RSC Advances. 2014;4(28):14441-14446.
15. Ou J, Wang F, Huang Y, et al. Fabrication and cyto-compatibility of Fe_3O_4/SiO_2/graphene-CdTe QDs/CS nanocomposites for drug delivery. Colloids Surf B Biointerfaces. 2014;117:466-472.
16. Liu MM, Sun J. In situ growth of monodisperse Fe_3O_4 nanoparticles on graphene as flexible paper for supercapacitor. Journal of Materials Chemistry A. 2014;2(30):12068-12074.
17. He H, Gao C. Supraparamagnetic, conductive, and processable multifunctional graphene nanosheets coated with high-density Fe_3O_4 nanoparticles. ACS Appl Mater Interfaces. 2010;2(11):3201-3210.
18. Liang JJ, Xu YF, Sui D, et al. Flexible, magnetic, and electrically conductive graphene/Fe_3O_4 paper and its application for magnetic-controlled switches. J Phys Chem C. 2010;114(41):17465-17471.
19. Narayanan TN, Liu Z, Lakshmy PR, et al. Synthesis of reduced graphene oxide-Fe_3O_4 multifunctional freestanding membranes and their temperature dependent electronic transport properties. Carbon. 2012;50(3):1338-1345.
20. Hummers WS Jr, Offeman RE. Preparation of graphitic oxide. J Am Chem Soc. 1958;80(6):1339-1339.
21. Zangmeister CD. Preparation and evaluation of graphite oxide reduced at 220°C. Chem Mater. 2010;22(19):5625-5629.
22. Xiao M, Du XS, Meng YZ, Gong KC. The influence of thermal treatment conditions on the structures and electrical conductivities of graphite oxide. New Carbon Materials. 2004;19(2):92-96.
23. Jeong HK, Lee YP, Jin MH, Kim ES, Bae JJ, Lee YH. Thermal stability of graphite oxide. Chem Phys Lett. 2009;470(4-6):255-258.
24. Chen HQ, Mueller MB, Gilmore KJ, Wallace GG, Li D. Mechanically strong, electrically conductive, and biocompatible graphene paper. Adv Mater. 2008;20(18):3557-3561.
25. Cong HP, He JJ, Lu Y, Yu SH. Water-soluble magnetic-functionalized reduced graphene oxide sheets: in situ synthesis and magnetic resonance imaging applications. Small. 2010;6(2):169-173.
26. Xu Y, Sheng K, Li C, Shi G. Self-assembled graphene hydrogel via a one-step hydrothermal process. ACS Nano. 2010;4(7):4324-4330.
27. Tran Thanh T, Feller JF, Kim T, Kim H, Yang WS, Suh KS. Electromagnetic properties of Fe_3O_4-functionalized graphene and its composites with a conducting polymer. Journal of Polymer Science: Part a: Polymer Chemistry. 2012;50(5):927-935.
28. Wang TS, Liu ZH, Lu MM, et al. Graphene-Fe_3O_4 nanohybrids: synthesis and excellent electromagnetic absorption properties. J Appl Phys. 2013;113(2):024314.
29. Valles C, David Nunez J, Benito AM, Maser WK. Flexible conductive graphene paper obtained by direct and gentle annealing of graphene oxide paper. Carbon. 2012;50(3):835-844.